

# Structural, Magnetic and Electrical Properties of One-dimensioal Tetraamidatodiruthenium Compounds

Patricia Delgado-Martínez,<sup>a</sup> Rodrigo González-Prieto,<sup>a</sup> Carlos J. Gómez-García,\*<sup>b</sup> Reyes Jiménez-Aparicio,\*<sup>a</sup> José L. Priego,<sup>a</sup> and Rosario M. Torres.<sup>c</sup>

<sup>a</sup>Departamento de Química Inorgánica, Facultad de Ciencias Químicas, Universidad Complutense de Madrid, Ciudad Universitaria, E-28040 Madrid, Spain. E-mail: reyesja@quim.ucm.es

<sup>b</sup>Instituto de Ciencia Molecular. Parque Científico. Universidad de Valencia. C/ Catedrático José Beltrán, 2. 46980 Paterna Valencia, Spain. E-mail: carlos.gomez@uv.es

<sup>c</sup>Centro de Asistencia a la Investigación de Rayos X. Facultad de Ciencias Químicas. Universidad Complutense de Madrid. Ciudad Universitaria, 28040 Madrid, Spain.

## Electronic Supplementary Information

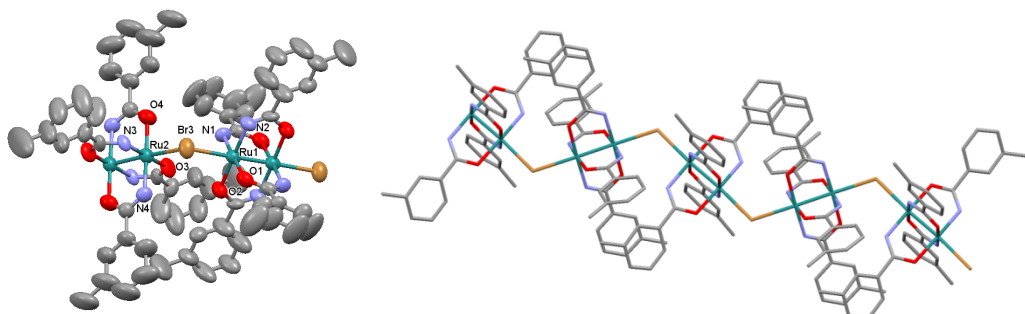


**Figure S1.** Left: thermal-ellipsoid representation of the paddlewheel monomer  $[\text{Ru}_2\text{Br}(\mu\text{-NHOCC}_6\text{H}_4\text{-}m\text{-Me})_4]$  (2), (50% probability ellipsoids). Right: zigzag  $[\text{Ru}_2\text{Br}(\mu\text{-NHOCC}_6\text{H}_4\text{-}m\text{-Me})_4]_n$  chain. Hydrogen atoms are omitted in both cases for clarity.

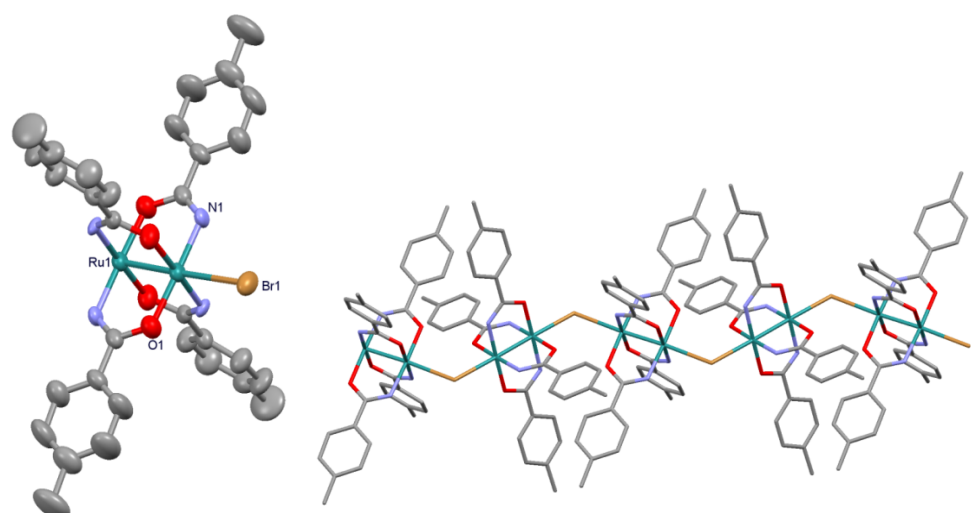


**Figure S2.** Left: thermal-ellipsoid representation of the paddlewheel monomer  $[\text{Ru}_2\text{Br}(\mu\text{-NHOCC}_6\text{H}_4\text{-p-Me})_4]$  (3), (50% probability ellipsoids). Right: zigzag  $[\text{Ru}_2\text{Br}(\mu\text{-NHOCC}_6\text{H}_4\text{-p-Me})_4]_n$  chain. Hydrogen atoms are omitted in both cases for clarity.

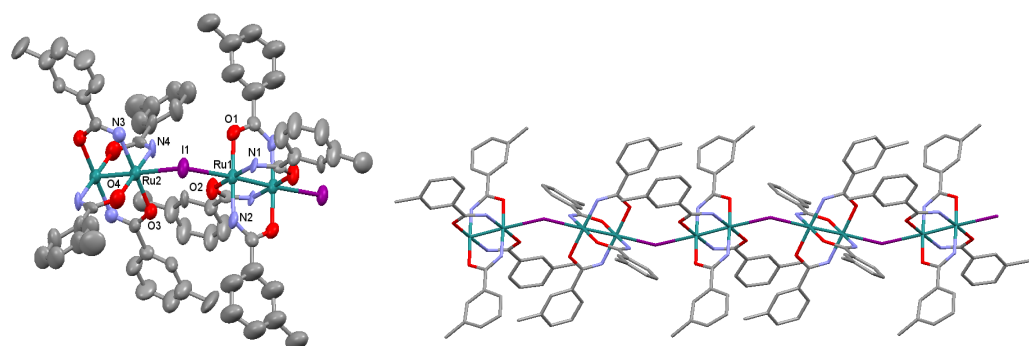


**Figure S3.** Left: thermal-ellipsoid representation of the paddlewheel monomer  $[\text{Ru}_2\text{I}(\mu\text{-NHOCC}_6\text{H}_4\text{-m-Me})_4]$  (5), (50% probability ellipsoids). Right: zigzag  $[\text{Ru}_2\text{I}(\mu\text{-NHOCC}_6\text{H}_4\text{-m-Me})_4]_n$  chain. Hydrogen atoms are omitted in both cases for clarity.

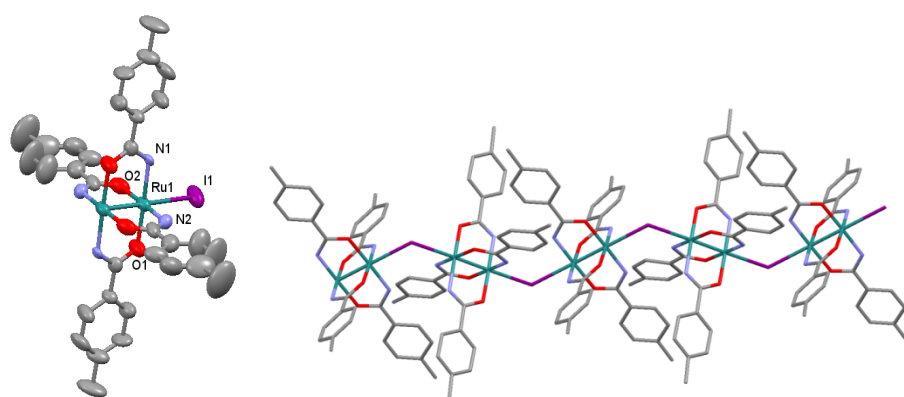


**Figure S4.** Left: thermal-ellipsoid representation of the paddlewheel monomer  $[\text{Ru}_2\text{I}(\mu\text{-NHOCC}_6\text{H}_4\text{-p-Me})_4]$  (6), (50% probability ellipsoids). Right: zigzag  $[\text{Ru}_2\text{I}(\mu\text{-NHOCC}_6\text{H}_4\text{-p-Me})_4]_n$  chain. Hydrogen atoms are omitted in both cases for clarity.

**Table S1.** Electronic spectra data for compounds **1-6**.

Compound	Not assigned	$\sigma$ (axial ligand) $\rightarrow\pi^*(\text{Ru}_2)$	$\pi(\text{O/N})$ $\rightarrow\pi^*(\text{Ru}_2)$	$\pi(\text{RuO/N,Ru}_2)$ $\rightarrow\pi^*(\text{Ru}_2)$	$\sigma(\text{Ru-axial ligand})$ $\rightarrow\pi^*(\text{Ru}_2)$	$\delta(\text{Ru}_2)$ $\rightarrow\delta^*(\text{Ru}_2)$
<b>1</b>	270	289	401	481	555sh	921
<b>2</b>	269	302	365sh	475	-	985
<b>3</b>	275sh	303	377	471	-	997
<b>4</b>	267	331	388	492	550sh	972
<b>5</b>	274	339	379	492	-	991
<b>6</b>	278	342	375	486	-	1007

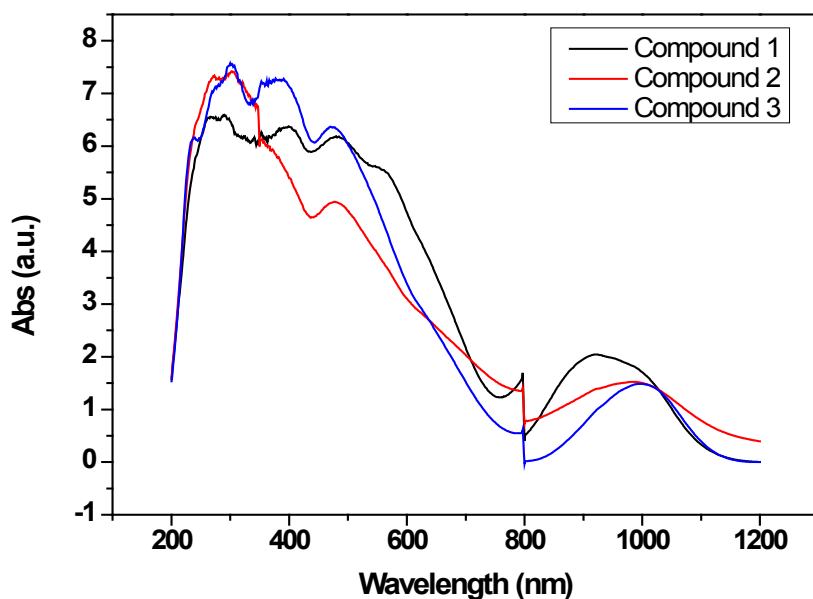


**Figure S5.** Electronic spectra of compounds **1-3** measured by diffuse reflectance. The reflectance data were treated with Kubelka-Munt correction.

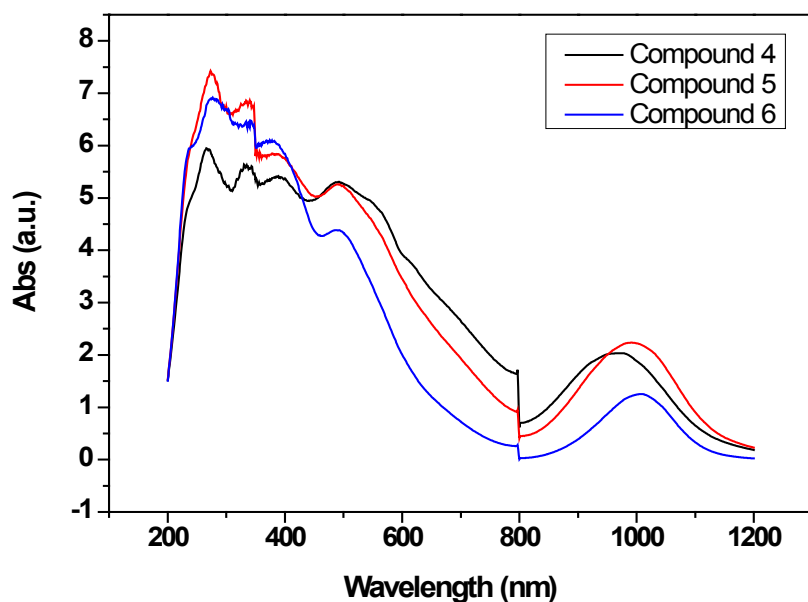


**Figure S6.** Electronic spectra of compounds 4-6 measured by diffuse reflectance. The reflectance data were treated with Kubelka-Munt correction.

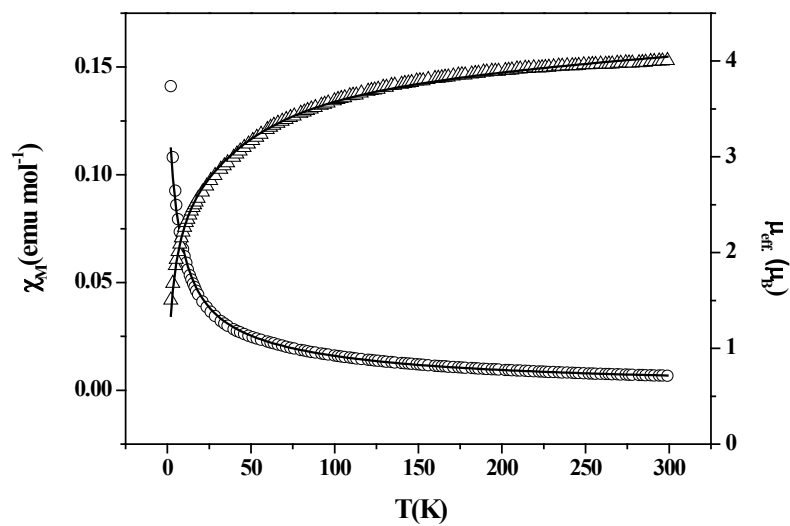


**Figure S7.** Thermal variation of the molar susceptibility  $\chi_m$  (circles) and  $\mu_{\text{eff.}}$  (triangles) for complex 3. Solid lines are the best fit to the model indicated in the text.

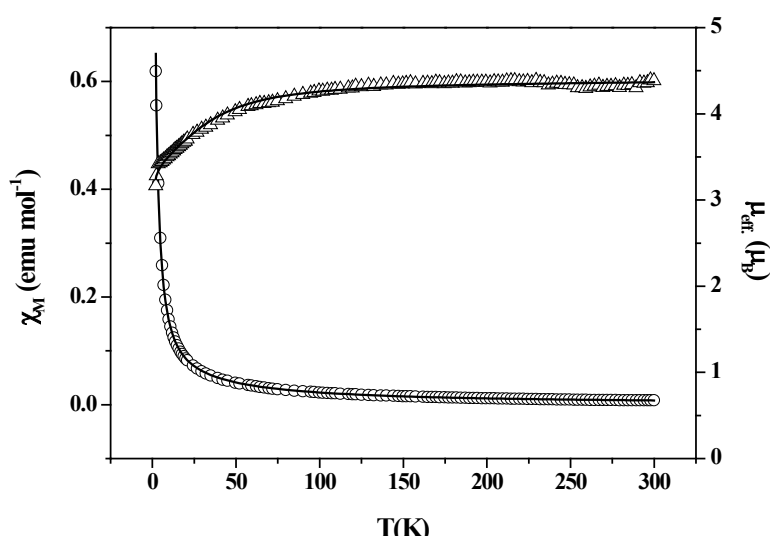


**Figure S8.** Thermal variation of the molar susceptibility  $\chi_m$  (circles) and  $\mu_{\text{eff}}$  (triangles) for complex 4. Solid lines are the best fit to the model indicated in the text.

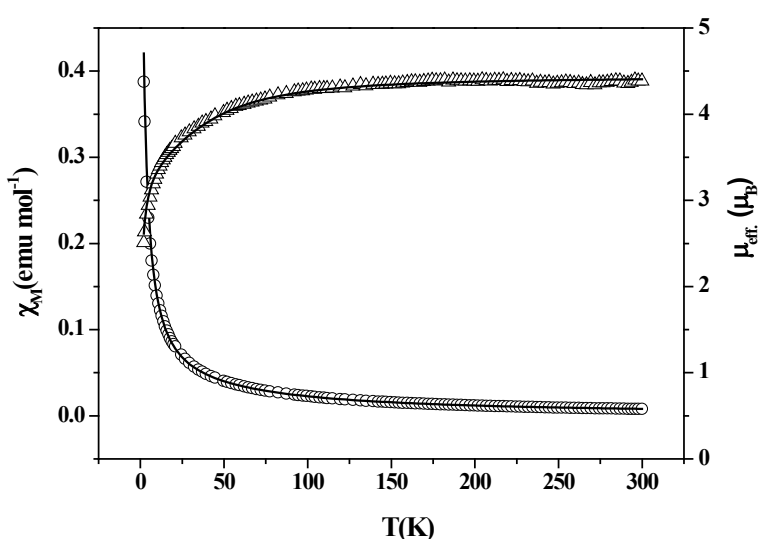


**Figure S9.** Thermal variation of the molar susceptibility  $\chi_m$  (circles) and  $\mu_{\text{eff}}$  (triangles) for complex 5. Solid lines are the best fit to the model indicated in the text.

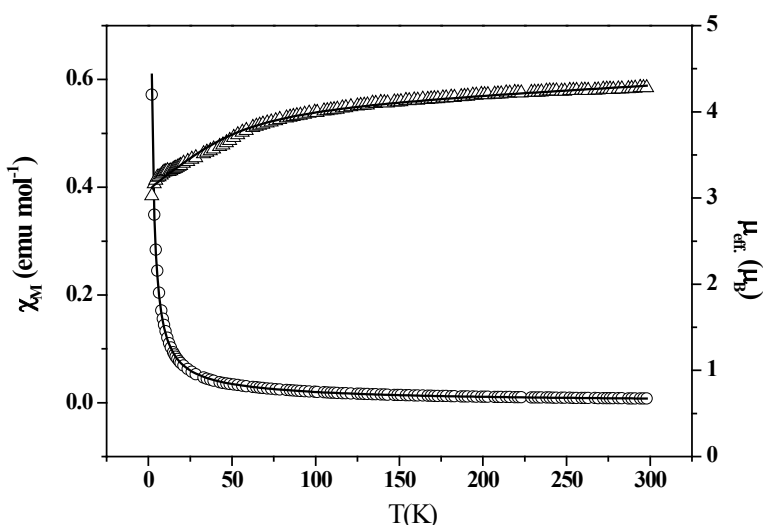


**Figure S10.** Thermal variation of the molar susceptibility  $\chi_m$  (circles) and  $\mu_{eff}$  (triangles) for complex 6. Solid lines are the best fit to the model indicated in the text.

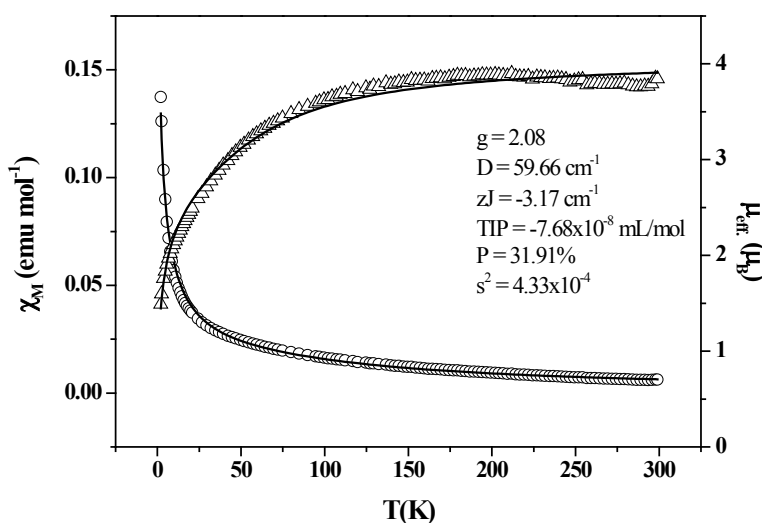


**Figure S11.** Thermal variation of the molar susceptibility  $\chi_m$  (circles) and  $\mu_{eff}$  (triangles) for complex 1. Solid lines are the best fit to the model considering a linear polymorph as paramagnetic impurity.

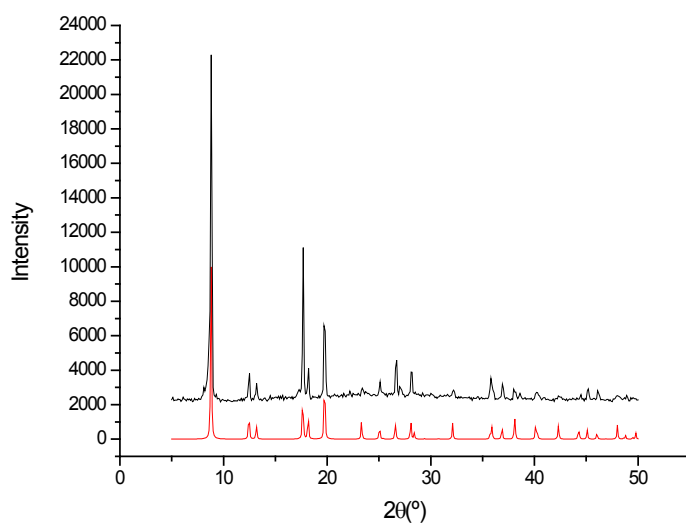


**Figure S12.** Experimental powder X-Ray diffractogram for compound 1 (Black), Simulated diffractogram obtained from single crystal X-ray determination (Red).

**Table S2.** Crystal data and Refinement Data for  $\text{Ru}_2\text{Br}(\mu\text{-NHOCC}_6\text{H}_4\text{-Me})_4\text{]}_n$  (**1-3**).

Crystal Data	1	2	3
<b>Empirical formula</b>	$\text{C}_{32}\text{H}_{32}\text{BrN}_4\text{O}_4\text{Ru}_2$	$\text{C}_{32}\text{H}_{32}\text{BrN}_4\text{O}_4\text{Ru}_2$	$\text{C}_{32}\text{H}_{32}\text{BrN}_4\text{O}_4\text{Ru}_2$
<b>Formula wt</b>	818.67	818.67	818.67
<b>Crystal system.</b>	Tetragonal	Monoclinic	Monoclinic
<b>Space group</b>	I-4/m	P2(1)/c	C2/c
<i>a</i> /Å	14.203(2)	13.092(2)	26.942(6)
<i>b</i> /Å	14.203(2)	11.138(2)	10.424(2)
<i>c</i> /Å	7.6293(13)	22.418(5)	13.010(2)
$\alpha/^\circ$	90.0	90.0	90.0
$\beta/^\circ$	90.0	97.86(3)	113.32(3)
$\gamma/^\circ$	90.0	90.0	90.0
<i>V</i> /Å <sup>3</sup>	1539.1(4)	3235.8(11)	3355.4(12)
<b>Z</b>	2	4	4
<b>D<sub>c</sub>/g/cm<sup>3</sup></b>	1.767	1.680	1.621
$\mu(\text{Mo-K}\alpha)/\text{mm}^{-1}$	2.323	2.210	2.131
<b>F(000)</b>	814	1628	1628
<b>θ range/°</b>	2.03 to 26.96	1.57 to 25.00	1.65 to 27.00
<b>index ranges</b>	-14,-18,-9 to 18, 18, 9	-15,-12,-24 to 15, 13, 26	-34,-13,-16 to 31, 13, 16
<b>reflections collected</b>	6945	23913	14504
<b>unique reflections</b>	916	5699	3669
<b>[Rint]</b>	[Rint = 0.0335]	[R(int) = 0.0673]	[R(int) = 0.0524]
<b>completeness to theta</b>	100%	99.7%	99.7%
<b>data/restraints/params</b>	916/0/59	5699/32/322	3669/0/195
<b>Goodness-of-fit on F<sup>2</sup></b>	0.992	1.010	0.999
<b>R1 (reflns obsd)</b>	0.0323(829)	0.0966(2965)	0.0441(2297)
<b>[I&gt;2σ(I)]<sup>a</sup></b>			
<b>wR2 (all data)<sup>b</sup></b>	0.1023	0.3303	0.1659

<sup>a</sup>  $R1 = \sum ||F_o - |F_c|| / \sum |F_o|$

<sup>b</sup>  $wR2 = \{\sum [w(F_o^2 - F_c^2)^2] / \sum [w(F_o^2)^2]\}$

**Table S3.** Crystal data and Refinement Data for Ru<sub>2</sub>I(μ-NHOCC<sub>6</sub>H<sub>4</sub>-Me)<sub>4</sub>]<sub>n</sub> (**4-6**).

Crystal Data	<b>4</b>	<b>5</b>	<b>6</b>
<b>Empirical formula</b>	C <sub>32</sub> H <sub>32</sub> IN <sub>4</sub> O <sub>4</sub> Ru <sub>2</sub>	C <sub>32</sub> H <sub>32</sub> IN <sub>4</sub> O <sub>4</sub> Ru <sub>2</sub>	C <sub>32</sub> H <sub>32</sub> IN <sub>4</sub> O <sub>4</sub> Ru <sub>2</sub>
<b>Formula wt</b>	865.66	865.66	865.66
<b>Crystal system.</b>	Triclinic	Monoclinic	Monoclinic
<b>Space group</b>	P-1	P2(1)/c	I2/a
<i>a</i> /Å	11.8852(7)	11.076(2)	13.470(4)
<i>b</i> /Å	13.4489(8)	22.551(4)	18.229(6)
<i>c</i> /Å	20.697(1)	13.443(2)	15.637(7)
$\alpha$ /°	94.477(1)	90.0	90.0
$\beta$ /°	94.735(1)	95.303(4)	110.823(7)
$\gamma$ /°	90.345(1)	90.0	90.0
<i>V</i> /Å <sup>3</sup>	3286.7(3)	3343.5(11)	3589(2)
<i>Z</i>	4	4	4
D <sub>c</sub> /g/cm <sup>3</sup>	1.749	1.720	1.602
$\mu$ (Mo-Kα)/mm <sup>-1</sup>	1.899	1.867	1.739
F(000)	1700	1700	1700
$\theta$ range/°	1.52 to 25.00	1.77 to 25.00	1.79 to 25.00
index ranges	-14,-15,-21 to 12, 15, 24	-13,-26,-15 to 12, 27, 15	-15,-20,-18 to 15, 21, 13
reflections collected	25323	24955	9904
unique reflections	11265	5874	3143
[Rint]	[Rint = 0.0519]	[R(int) = 0.1231]	[R(int) = 0.1222]
completeness to theta	97.2%	99.8%	99.1%
data/restraints/params	11265/0/764	5874/8/316	3143/0/183
Goodness-of-fit on F <sup>2</sup>	0.993	1.075	1.084
R1 (reflns obsd)	0.0423(6817)	0.0805(2903)	0.0815(1540)
[I>2σ(I)] <sup>a</sup>			
wR2 (all data) <sup>b</sup>	0.1050	0.2893	0.2959

<sup>a</sup> R1 =  $\sum ||F_o| - |F_c|| / \sum |F_o|$

<sup>b</sup> wR2 = { $\sum [w(F_o^2 - F_c^2)^2] / \sum [w(F_o^2)^2]$ }

### Correlation between Magnetic and Structural Parameters

Since, including the six compounds (**1-6**) reported in this manuscript, there is a total of twenty three magnetically and structurally characterized chains compounds of the type  $[\text{Ru}_2\text{X}(\mu\text{-L-L})_4]$  ( $\text{X}$  = halide,  $\mu\text{-L-L}$  = carboxylate or amidate), we have tried to perform a direct magneto-structural correlation between the magnetic parameters ( $|D|$  and  $zJ$ ) and the, probably most important structural parameters (the Ru-X-Ru bond angle and the Ru-X bond length). As expected, the  $|D|$  parameter is not related with this angle (figure S13) but the  $zJ$  coupling follows an approximate linear correlation with the Ru-X-Ru bond angle (figure S14). Figure S14 shows that, as expected, as the Ru-X-Ru bond angle increases, the (antiferro)magnetic coupling increases, reaching a maximum value for Ru-X-Ru bond angles of  $180^\circ$ . Note that in all the correlations presented, compound **20** correlated much worse than the others. This is probably due to the fact that in this compound the  $D$  parameter is significantly smaller and, therefore, the antiferromagnetic coupling has to be larger since both parameters are responsible of the decrease observed in  $\chi_m\text{T}$  at low temperatures. We should, therefore, exclude compound **20** from all the correlations.

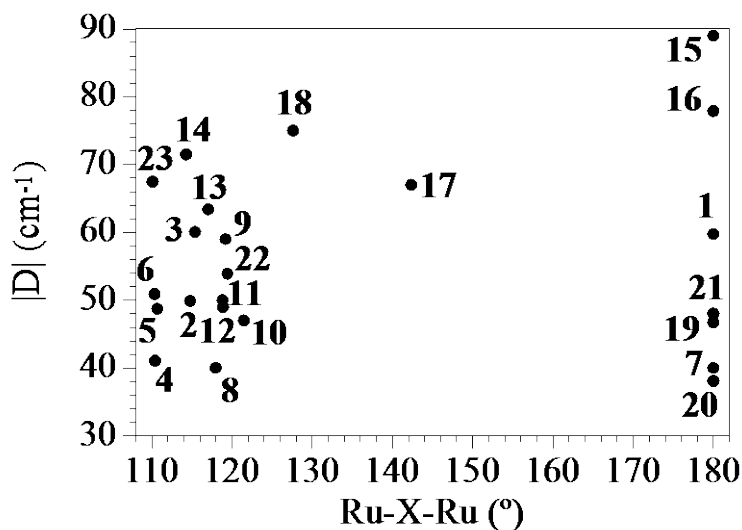


**Figure S13.** Variation of  $|D|$  as a function of the Ru-X-Ru bond angle in all the magnetically and structurally characterized chains compounds of the type  $[\text{Ru}_2\text{X}(\mu\text{-L-L})_4]$  ( $\text{X}$  = halide,  $\mu\text{-L-L}$  = carboxylate or amidate) showing the lack of any correlation between these two parameters. The numbers of the compounds correspond to those displayed in table S4.

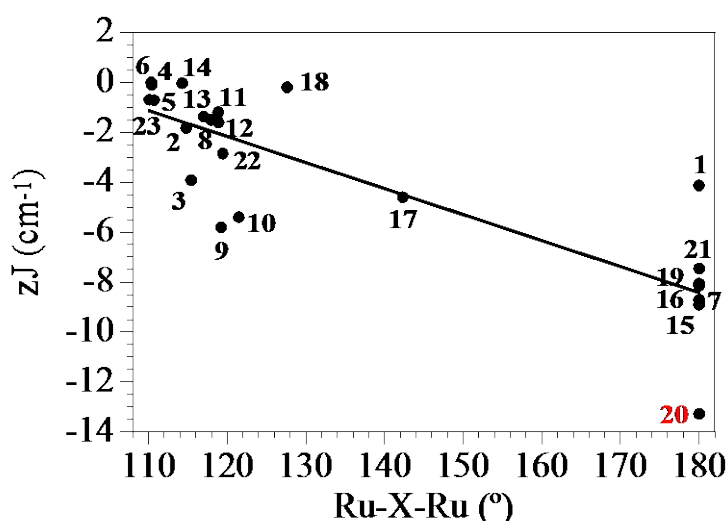


**Figure S14.** Variation of  $zJ$  as a function of the Ru-X-Ru bond angle in all the magnetically and structurally characterized chains compounds of the type  $[Ru_2X(\mu-L-L)_4]$  ( $X$  = halide,  $\mu$ -L-L = carboxylate or amide). Solid lines are the best linear fits to the points displayed in each plot. The numbers of the compounds correspond to those displayed in table S4.

The lack of a very precise linear correlation is probably due to the fact that other structural parameters, as the Ru-X bond length, must also play a very important role in determining the magnetic coupling. In fact, as can be seen in figures S15 and S16, although, as expected, the  $|D|$  parameter shows no correlation with the Ru-X bond length (figure S15), the  $zJ$  coupling shows an approximate linear correlation where the coupling decreases as the Ru-X bond length decreases (figure S16). Note that again the main discrepancy is shown by compound 20, where the coupling is stronger than expected.

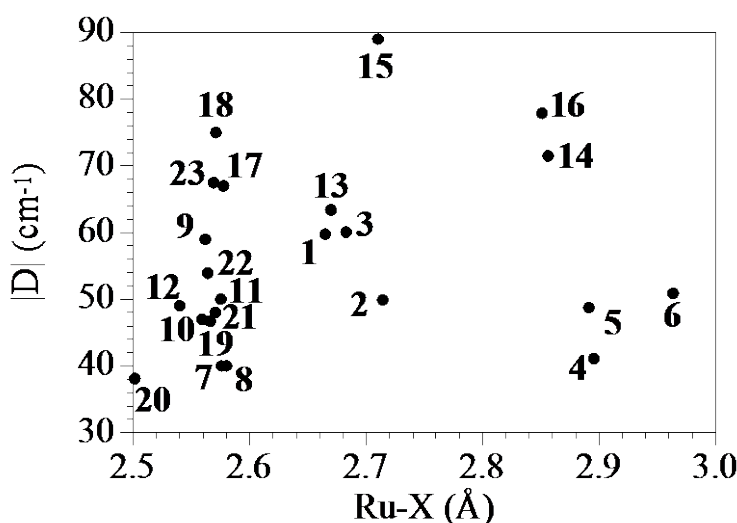


**Figure S15.** Variation of  $|D|$  as a function of the Ru-X bond length in all the magnetically and structurally characterized chains compounds of the type  $[Ru_2X(\mu-L-L)_4]$  ( $X$  = halide,  $\mu$ -L-L = carboxylate or amide) showing the lack of any correlation between these two parameters.

The numbers of the compounds correspond to those displayed in table S4.

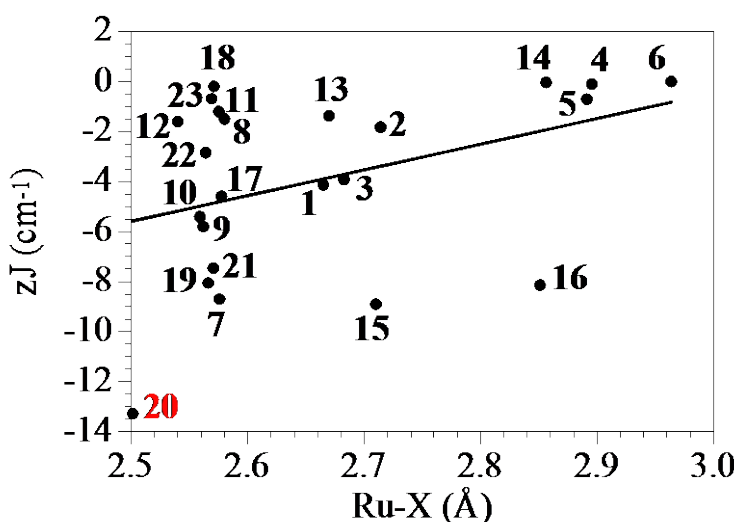


**Figure S16.** Variation of  $zJ$  as a function of the Ru-X bond length in all the magnetically and structurally characterized chains compounds of the type  $[Ru_2X(\mu-L-L)_4]$  ( $X$  = halide,  $\mu$ -L-L = carboxylate or amidate). Solid line is the best linear fit to the points. The numbers of the compounds correspond to those displayed in table S4.

Finally, in order to include both parameters (Ru-X bond length and Ru-X-Ru bond angle), we have established a correlation between the two magnetic parameters,  $|D|$  and  $zJ$  with the ratio between the Ru-X bond length and the Ru-X-Ru bond angle. Again, the  $|D|$  parameter shows no correlation (Figure S17) but the magnetic coupling  $zJ$  shows a linear correlation where, as expected, the coupling increases as the Ru-X/Ru-X-Ru ratio decreases (i.e., as the Ru-X decreases and the Ru-X-Ru angle increases) (Figure S18).

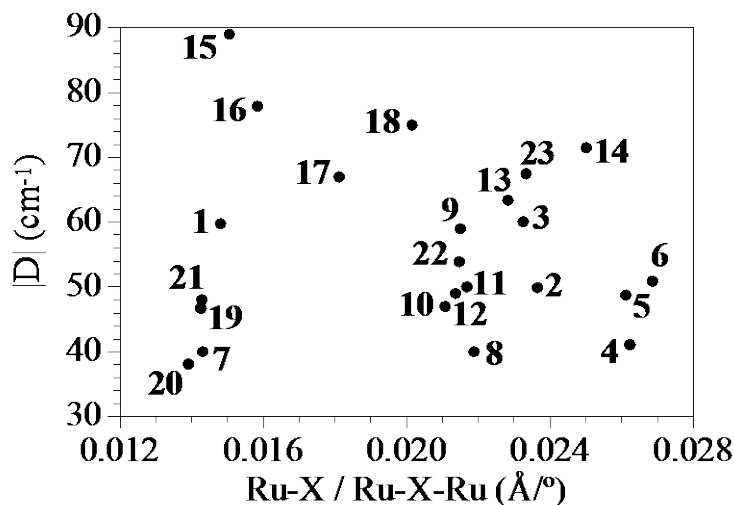


**Figure S17.** Variation of  $|D|$  as a function of the Ru-X/Ru-X-Ru ratio in all the magnetically and structurally characterized chains compounds of the type  $[Ru_2X(\mu-L-L)_4]$  ( $X$  = halide,  $\mu$ -L-L = carboxylate or amidate) showing the lack of any correlation between these two parameters. The numbers of the compounds correspond to those displayed in table S4.

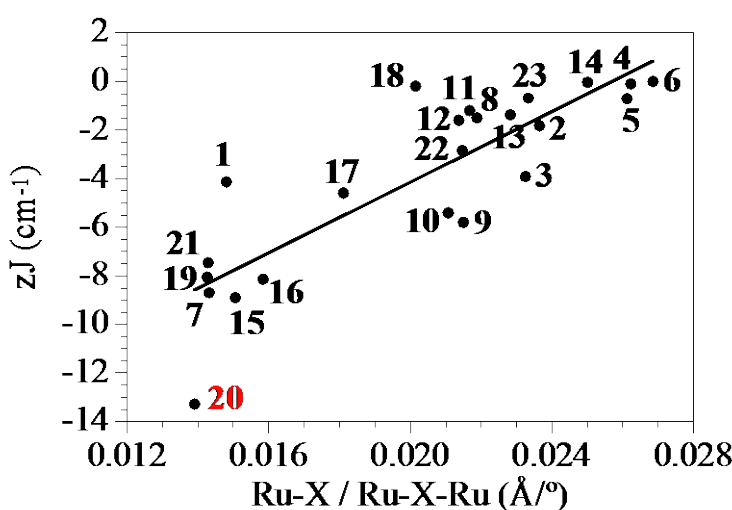


**Figure S18.** Variation of  $zJ$  as a function of the  $\text{Ru-X}/\text{Ru-X-Ru}$  ratio in all the magnetically and structurally characterized chains compounds of the type  $[\text{Ru}_2\text{X}(\mu\text{-L-L})_4]$  ( $\text{X} = \text{halide}$ ,  $\mu\text{-L-L} = \text{carboxylate or amidate}$ ). Solid line is the best linear fit to the points. The numbers of the compounds correspond to those displayed in table S4.

**Table S4.** Structural and magnetic parameters in all the magnetically and structurally characterized chain compounds of the type  $[\text{Ru}_2\text{X}(\mu\text{-L-L})_4]$  ( $\text{X} = \text{halide}$ ,  $\mu\text{-L-L} = \text{carboxylate or amidate}$ )

	Compound	$\text{Ru-X-Ru} (\circ)$	$\text{Ru-X} (\text{\AA})$	$ \mathbf{D}  (\text{cm}^{-1})$	$zJ (\text{cm}^{-1})$	Ref
1	$\text{Ru}_2\text{Br}(\mu\text{-NHOCC}_6\text{H}_4\text{-}o\text{-Me})_4$	180.00	2.6655	59.77	-4.13	this work
2	$\text{Ru}_2\text{Br}(\mu\text{-NHOCC}_6\text{H}_4\text{-}m\text{-Me})_4$	114.77	2.700 2.728	49.92	-1.82	this work
3	$\text{Ru}_2\text{Br}(\mu\text{-NHOCC}_6\text{H}_4\text{-}p\text{-Me})_4$	115.39	2.6829 2.6830	60.10	-3.92	this work
4	$\text{Ru}_2\text{I}(\mu\text{-NHOCC}_6\text{H}_4\text{-}o\text{-Me})_4$	110.67 110.16	2.8908 2.8517 2.8950 2.9447	41.10	-0.09	this work
5	$\text{Ru}_2\text{I}(\mu\text{-NHOCC}_6\text{H}_4\text{-}m\text{-Me})_4$	110.67	2.9085 2.8741	48.76	-0.71	this work
6	$\text{Ru}_2\text{I}(\mu\text{-NHOCC}_6\text{H}_4\text{-}p\text{-Me})_4$	110.35	2.9636	50.95	0.0	this work
7	$\text{Ru}_2\text{Cl}(\mu\text{-NHOCC}_6\text{H}_4\text{-}o\text{-Me})_4$	180.00	2.5756	40	-8.7	1
8	$\text{Ru}_2\text{Cl}(\mu\text{-NHOCC}_6\text{H}_4\text{-}m\text{-Me})_4$	117.93	2.563 2.597	40	-1.5	1
9	$\text{Ru}_2\text{Cl}(\mu\text{-NHOCC}_6\text{H}_4\text{-}p\text{-Me})_4$	119.20	2.562	59	-5.8	1
10	$\text{Ru}_2\text{Cl}(\mu\text{-O}_2\text{CC}_6\text{H}_4\text{-}o\text{-Me})_4$	121.45	2.559	47	-5.4	1
11	$\text{Ru}_2\text{Cl}(\mu\text{-O}_2\text{CC}_6\text{H}_4\text{-}m\text{-Me})_4$	118.80	2.565 2.585	50	-1.2	1
12	$\text{Ru}_2\text{Cl}(\mu\text{-O}_2\text{CC}_6\text{H}_4\text{-}p\text{-Me})_4$	118.88	2.5400	49	-1.6	1
13	$\text{Ru}_2\text{Br}(\mu\text{-O}_2\text{CPh})_4$	117.00	2.6700	63.4	-1.37	2
14	$\text{Ru}_2\text{I}(\mu\text{-O}_2\text{CPh})_4$	114.25	2.8562	71.5	-0.03	2
15	$\text{Ru}_2\text{Br}(\mu\text{-O}_2\text{CEt})_4$	180.00	2.7101	89	-8.9	3
16	$\text{Ru}_2\text{I}(\mu\text{-O}_2\text{CEt})_4$	180.00	2.851	77.89	-8.14	4
17	$\text{Ru}_2\text{Cl}(\mu\text{-O}_2\text{CBu}^n)_4$	142.30	2.5774	67	-4.6	5
18	$\text{Ru}_2\text{Cl}(\mu\text{-O}_2\text{CMe})_4$	127.60	2.571	75	-0.19	5, 6
19	$\text{Ru}_2\text{Cl}(\mu\text{-O}_2\text{CEt})_4$	180.00	2.566	46.7	-8.05	7, 8
20	$\text{Ru}_2\text{Cl}(\mu\text{-O}_2\text{CCMePh}_2)_4$	180.00	2.5016	38.1	-13.28	8, 9
21	$\text{Ru}_2\text{Cl}(\mu\text{-O}_2\text{CCMe=CHEt})_4$	180.00	2.5705	48	-7.46	8, 10
22	$\text{Ru}_2\text{Cl}(\mu\text{-O}_2\text{CCH=CHCH=CHMe})_4$	119.43	2.564	53.9	-2.84	11
23	$\text{Ru}_2\text{Cl}(\mu\text{-O}_2\text{CCH}_2\text{OMe})_4$	110.11	2.569	67.5	-0.69	11

- [1] P. Delgado, R. González-Prieto, R. Jiménez-Aparicio, J. Perles, J. L. Priego, M. R. Torres, *Dalton Trans.*, 2012, **41**, 11866.
- [2] M. C. Barral, R. González-Prieto, R. Jiménez-Aparicio, J. L. Priego, M. R. Torres and F. A. Urbanos, *Eur. J. Inorg. Chem.*, 2004, 4491.
- [3] D. Olea, R. González-Prieto, J. L. Priego, M. C. Barral, P. J. Pablo, M. R. Torres, J. Gómez-Herrero, R. Jiménez-Aparicio and F. Zamora, *Chem. Commun.*, 2007, 1591.
- [4] L. Welte, R. González-Prieto, D. Olea, M. R. Torres, J. L. Priego, R. Jiménez-Aparicio, J. Gómez-Herrero and F. Zamora, *ACS Nano*, 2008, **2**, 2051.
- [5] F. D. Cukiernik, D. Luneau, J.-C. Marchon and P. Maldivi, *Inorg. Chem.*, 1998, **37**, 3698.
- [6] T. Togano, M. Mukaida, T. Nomura, *Bull. Chem. Soc. Jpn.* 1980, **53**, 2085.
- [7] A. Bino, F. A. Cotton and T. R. Felthouse, *Inorg. Chem.*, 1979, **18**, 2599.
- [8] R. Jiménez-Aparicio, F. A. Urbanos and J. M. Arrieta, *Inorg. Chem.*, 2001, **40**, 613.
- [9] F. A. Cotton, Y. Kim and T. Ren, *Polyhedron*, 1993, **12**, 607.
- [10] M.C. Barral, R. Jiménez-Aparicio, D. Pérez-Quintanilla, E. Pinilla, J. L. Priego, E. C. Royer, F. A. Urbanos, *Polyhedron*, 1998, **18**, 371.
- [11] M. C. Barral, R. Jiménez-Aparicio, D. Pérez-Quintanilla, J. L. Priego, E. C. Royer, M. R. Torres, F. A. Urbanos, *Inorg. Chem.*, 2000, **39**, 65.